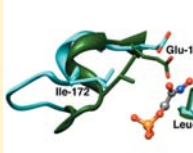
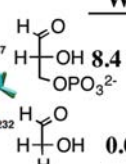


Mechanism for Activation of Triosephosphate Isomerase by Phosphite Dianion: The Role of a Hydrophobic Clamp

M. Merced Malabanan, Astrid P. Koudelka, Tina L. Amyes, and John P. Richard*

Department of Chemistry, University at Buffalo, the State University of New York, Buffalo, New York 14260-3000, United States

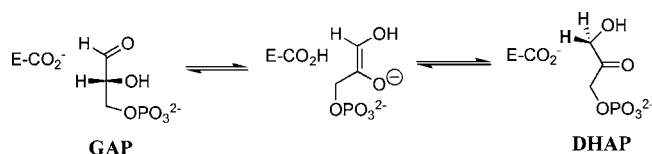
ABSTRACT: The role of the hydrophobic side chains of Ile-172 and Leu-232 in catalysis of the reversible isomerization of *R*-glyceraldehyde 3-phosphate (GAP) to dihydroxyacetone phosphate (DHAP) by triosephosphate isomerase (TIM) from *Trypanosoma brucei brucei* (*Tbb*) has been investigated. The I172A and L232A mutations result in 100- and 6-fold decreases in k_{cat}/K_m for the isomerization reaction, respectively. The effect of the mutations on the product distributions for the catalyzed reactions of GAP and of [$1\text{-}^{13}\text{C}$]-glycolaldehyde ([$1\text{-}^{13}\text{C}$]-GA) in D_2O is reported. The 40% yield of DHAP from wild-type *Tbb* TIM-catalyzed isomerization of GAP with intramolecular transfer of hydrogen is found to decrease to 13% and to 4%, respectively, for the reactions catalyzed by the I172A and L232A mutants. Likewise, the 13% yield of [$2\text{-}^{13}\text{C}$]-GA from isomerization of [$1\text{-}^{13}\text{C}$]-GA in D_2O is found to decrease to 2% and to 1%, respectively, for the reactions catalyzed by the I172A and L232A mutants. The decrease in the yield of the product of intramolecular transfer of hydrogen is consistent with a repositioning of groups at the active site that favors transfer of the substrate-derived hydrogen to the protein or the oxygen anion of the bound intermediate. The I172A and L232A mutations result in (a) a >10-fold decrease (I172A) and a 17-fold increase (L232A) in the second-order rate constant for the TIM-catalyzed reaction of [$1\text{-}^{13}\text{C}$]-GA in D_2O , (b) a 170-fold decrease (I172A) and 25-fold increase (L232A) in the third-order rate constant for phosphite dianion (HPO_3^{2-}) activation of the TIM-catalyzed reaction of GA in D_2O , and (c) a 1.5-fold decrease (I172A) and a larger 16-fold decrease (L232A) in K_d for activation of TIM by HPO_3^{2-} in D_2O . The effects of the I172A mutation on the kinetic parameters for the wild-type TIM-catalyzed reactions of the whole substrate and substrate pieces are consistent with a decrease in the basicity of the carboxylate side chain of Glu-167 for the mutant enzyme. The data provide striking evidence that the L232A mutation leads to a ca. 1.7 kcal/mol stabilization of a catalytically active loop-closed form of TIM (E_c) relative to an inactive open form (E_o).

Triosephosphate Isomerase	k_{cat}/K_m ($\text{M}^{-1} \text{s}^{-1}$)		
	WT	L232A	I172A
	8.4×10^6	1.5×10^6	8.0×10^4
	0.07	1.2 (!)	< 0.003

INTRODUCTION

Triosephosphate isomerase (TIM) is the prototypical protein catalyst of proton transfer at α -carbonyl carbon.^{1–5} This small protein (dimer, 26 kDa/subunit) catalyzes the reversible 1,2-shift of the *pro-R* proton at dihydroxyacetone phosphate (DHAP) to give (*R*)-glyceraldehyde 3-phosphate (GAP) by a single-base proton transfer mechanism through an enzyme-bound *cis*-enediolate intermediate (Scheme 1).^{1,6} The most important

Scheme 1



metabolic role for TIM is to enable DHAP, a product of aldolase-catalyzed cleavage of fructose 1,6-bisphosphate, to enter glycolysis. The enzyme has the more general “housekeeping” function of maintaining rapid equilibrium between GAP and DHAP so that these compounds are available, as needed, for glycolysis, the glycerol-3-phosphate shuttle, and the pentose phosphate pathway.⁷ Deficiencies in TIM are recognized as a recessive genetic disease associated with chronic hemolytic

anemia and progressive neuromuscular dysfunction that often result in early childhood death.^{7,8}

The chemical mechanism for TIM-catalyzed isomerization of triosephosphates was established by the early 1990s (Figure 1).

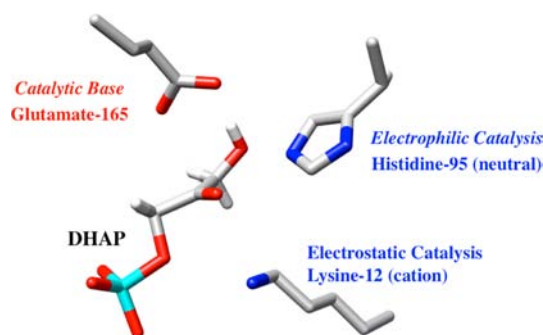


Figure 1. The orientation of the catalytic side chains at the active site of TIM from yeast [PDB entry 1NEY].

Isomerization at the active site of TIM is similar to nonenzymatic isomerization in water.⁹ Catalysis proceeds by deprotonation of

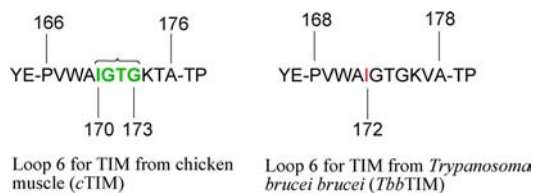
Received: April 17, 2012

Published: May 13, 2012

the bound substrate using the carboxylate side chain of Glu-165^{10,11} and is assisted by the neutral electrophilic imidazole side chain of His-95.^{12,13} The alkylammonium side chain of Lys-12 plays an important electrostatic role in stabilizing the negatively charged bound substrate and transition state.^{14–17} We have proposed that the functional groups of these side chains are activated for catalysis compared with the corresponding groups in water.^{5,18} We present here the results of experiments designed to probe the mechanism for side-chain activation.

Binding interactions between TIM and the phosphodianion group of GAP account for 80% of the ca. 14 kcal/mol enzymatic stabilization of the transition state for deprotonation of carbon.¹⁹ Roughly one-half of this binding energy is recovered in phosphite dianion (HPO_3^{2-}) activation of TIM for catalysis of deprotonation of the truncated substrate glycolaldehyde.²⁰ High-resolution X-ray crystal structures of complexes between TIM and substrate DHAP²¹ or between TIM and the tight-binding inhibitors phosphoglycolate (PGA)²² and phosphoglycolohydroxamate (PGH)^{23,24} show that the phosphodianion binding interactions are utilized to drive a large conformational change of the enzyme, the most prominent feature of which is closure of flexible loop 6 (residues 166–176 for TIM from chicken muscle, Scheme 2)

Scheme 2



over the enzyme active site.^{21,25–27} The deletion of residues 170–173 (green in Scheme 2) and the introduction of a peptide bond between Ala-169 and Lys-174 disrupt the loop–dianion interactions without significantly affecting the protein fold. This results in a substantial 10^5 -fold decrease in k_{cat} and a 2.3-fold increase in K_m for isomerization of GAP,²⁸ which serve as direct evidence that interactions between loop 6 and the substrate dianion activate TIM for catalysis.

Wierenga has provided a lucid and detailed description of the many changes in protein structure observed to occur upon ligand binding to TIM.^{4,29} The closure of loop 6 of TIM from *Trypanosoma brucei brucei* (*Tbb*TIM, residues 168–178 shown in Scheme 2) over bound PGA results in movement of the hydrophobic side chain of Ile-172 [Ile-170 for *c*TIM] toward the carboxylate side chain of Glu-167 and “drives” this anionic side chain toward the hydrophobic side chain of Leu-232 [Leu-230 for *c*TIM], which maintains a nearly fixed position (Figure 2A).²² The result is to sandwich the carboxylate anion between the hydrophobic side chains of Ile-172 and Leu-232 and to shield the anion from interactions with the aqueous solvent (Figure 2B).^{22,23,30} At the same time, loop closure extrudes several water molecules to the bulk solvent. Desolvation of the active site should result in an increase in the basicity of the carboxylate side chain that will activate the side chain for deprotonation of bound substrate.^{5,18} This analysis suggests that the greasy side chains of Ile-172 and Leu-232 of *Tbb*TIM play a critical role in TIM-catalyzed deprotonation of carbon.

We recently reported the surprising result that the L232A mutation of *Tbb*TIM, which we thought would be crippling, instead causes a 17-fold increase in the second-order rate constant for enzyme-catalyzed deprotonation of the truncated

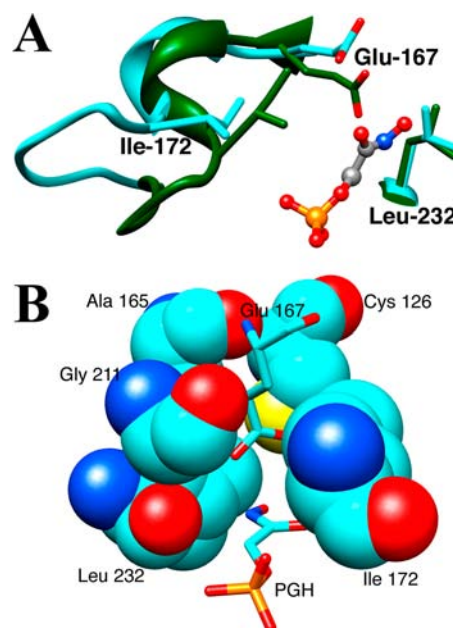


Figure 2. (A) Models from X-ray crystal structures of the unliganded open (cyan, PDB entry 5TIM) and PGH-liganded closed (green, PDB entry 1TRD) forms of TIM from *Trypanosoma brucei brucei* in the region of the enzyme active site. Closure of loop 6 (residues 168–178, Scheme 2) over the bound phosphodianion ligand results in movement of the hydrophobic side chain of Ile-172 toward the carboxylate side chain of the catalytic base Glu-167. This is accompanied by movement of Glu-167 toward the hydrophobic side chain of Leu-232, which maintains a nearly fixed position. (B) A structure that shows the positions of Ile-172 and Leu-232 at the active site “hydrophobic cage” for wild-type *Trypanosoma brucei* TIM in complex with PGH (PDB entry 1TRD).

substrate glycolaldehyde!³¹ Additional kinetic data reported for the catalyzed reactions of the substrate pieces glycolaldehyde and HPO_3^{2-} support the conclusion that the L232A mutation results in the stabilization of a high-energy, catalytically active, loop-closed form of TIM by 1.7 kcal/mol relative to the inactive open form of TIM.³¹ We now report the results of an expanded study on the effect of I172A, I172V, and L232A mutations on the kinetic parameters and the products of TIM-catalyzed reactions of the whole substrates GAP and DHAP and the substrate pieces. We had envisioned similar functions for the hydrophobic side chains of Ile-172 and Leu-232 in the desolvation and “clamping” of the carboxylate side chain of Glu-167. However, we observe that the I172A and L232A mutations result in very different changes in the kinetic parameters of the wild-type *Tbb*TIM, which shows that the two clamping side-chains play different roles in catalysis.

EXPERIMENTAL SECTION

Materials. Rabbit muscle α -glycerol 3-phosphate dehydrogenase and glyceraldehyde 3-phosphate dehydrogenase were purchased from Sigma. These enzymes were exhaustively dialyzed against 20 mM triethanolamine buffer (pH 7.5) at 7 °C prior to their use in coupled enzyme assays. Bovine serum albumin (BSA) was from Roche. CM Sepharose Fast Flow was from GE Healthcare. D,L-Glyceraldehyde 3-phosphate diethyl acetal (barium salt), DHAP (lithium or magnesium salt), NADH (disodium salt), dithiothreitol (DTT), Dowex 50WX4-200R, triethanolamine hydrochloride (TEA-HCl), and imidazole were purchased from Sigma. NAD (free acid) was purchased from MP Biomedicals or Calzyme, and sodium phosphite (dibasic, pentahydrate) and hydrogen arsenate heptahydrate were from Fluka. Sodium

phosphite was dried under vacuum prior to use.²⁰ [$1\text{-}^{13}\text{C}$]-Glycolaldehyde ($[1\text{-}^{13}\text{C}]$ -GA, 99% enriched with ^{13}C at C-1, 0.09 M in water) was purchased from Omicron Biochemicals. Deuterium oxide (99% D) and deuterium chloride (35% w/w, 99.9% D) were from Cambridge Isotope Laboratories. The barium salt of D-glyceraldehyde 3-phosphate diethyl acetal was prepared according to a literature procedure.³² Imidazole was recrystallized from benzene. All other chemicals were reagent grade or better and were used without further purification.

Stock solutions of GAP and D,L-glyceraldehyde 3-phosphate (D,L-GAP) at pH 7.5 were prepared by hydrolysis of the corresponding diethyl acetals (barium salt) using Dowex 50WX4-200R (H^+ form) in boiling H_2O or D_2O as described previously.³³ The resulting solutions were stored at $-20\text{ }^\circ\text{C}$ and adjusted to the appropriate pH or pD by the addition of 1 M NaOH or 1 M NaOD before use in enzyme assays.

The pTIM plasmid that contains the gene for wild-type TIM from *Trypanosoma brucei brucei* (*Tbb*) was a generous gift from Professor Rik Wierenga. The L232A mutant of TIM was prepared as described in earlier work.³¹ Site-directed mutagenesis to introduce the I172A and I172V mutations was performed by following the Stratagene protocol and using *Pfu* ultrahigh fidelity DNA polymerase. The primers 5'-CCC-GTT-TGG-GCC-GCG-GGT-ACC-GGC-AAG-GTG-GCG-ACA-CC-3' and 5'-CCC-GTT-TGG-GCC-GTC-GGT-ACC-GGC-AAG-GTG-GCG-ACA-CC-3' were used to introduce the I172A and I172V mutations, respectively. The product of the PCR reaction in a volume of 30 μL was treated with 20 units of the restriction enzyme *DpnI* at 37 $^\circ\text{C}$ for 1 hour in order to degrade the methylated DNA. The *Escherichia coli* strain K802 was transformed with 1 μL of the *DpnI*-digested PCR product. Several colonies were selected, and the plasmid DNA was purified using the QIAprep Miniprep Kit from Qiagen. The DNA sequences of the genes for the I172A and I172V mutant enzymes were verified by sequencing at the Roswell Park Cancer Institute (Buffalo, NY).

The I172A, I172V, and L232A mutant enzymes were expressed using the *E. coli* BL21 pLysS strain grown in LB medium at 18 $^\circ\text{C}$ and the proteins were purified by a published protocol.³⁴ The enzymes obtained from chromatography over a CM Sepharose column were judged to be homogeneous by gel electrophoresis. The concentration of the protein was determined from the absorbance at 280 nm using the extinction coefficient of $3.5 \times 10^4\text{ M}^{-1}\text{ cm}^{-1}$ calculated using the ProtParam tool available on the ExPasy server.^{35,36}

Preparation of Solutions. Solution pH or pD was determined at 25 $^\circ\text{C}$ using an Orion model 720A pH meter equipped with a radiometer pHC4006-9 combination electrode that was standardized at pH 7.0 and 4.0 or pH 7.0 and 10.0 at 25 $^\circ\text{C}$. Values of pD were obtained by adding 0.40 to the observed reading of the pH meter.³⁷ Imidazole and phosphite buffers were prepared as described in previous work.^{20,38} Triethanolamine buffers at pH 7.5 were prepared by neutralization of the hydrochloride salt with 1 M NaOH. Solutions of $[1\text{-}^{13}\text{C}]$ -GA were prepared, and the concentration of this compound was determined as described in earlier work.²⁰

Enzyme Assays. All enzyme assays were carried out at 25 $^\circ\text{C}$. One unit of enzyme activity is defined as the amount of enzyme that converts 1 μmol of substrate to product in 1 minute under the specified reaction conditions. The change in the concentration of NADH was calculated from the change in absorbance at 340 nm using an extinction coefficient of $6220\text{ M}^{-1}\text{ cm}^{-1}$. α -Glycerol 3-phosphate dehydrogenase was assayed by monitoring the oxidation of NADH by DHAP, as described in earlier work.³³ Glyceraldehyde 3-phosphate dehydrogenase was assayed by monitoring the enzyme-catalyzed reduction of NAD^+ by GAP. The assay solution (1.0 mL) contained 30 mM TEA (pH 7.5, $I = 0.1$, NaCl), 1 mM NAD^+ , 2 mM GAP, 5 mM disodium hydrogen arsenate, 3 mM DTT, and 0.01% BSA.

The TIM-catalyzed isomerization of GAP was monitored by coupling the formation of DHAP to the oxidation of NADH catalyzed by α -glycerol 3-phosphate dehydrogenase.³⁹ The TIM-catalyzed isomerization of DHAP was monitored by coupling the formation of GAP to the reduction of NAD^+ catalyzed by glyceraldehyde 3-phosphate dehydrogenase.⁴⁰ The assay mixtures (1.0 mL) contained 30 mM TEA (pH 7.5, $I = 0.1$, NaCl), DHAP (0.15–5.0 mM), 1 mM NAD, sodium

arsenate (2–15 mM), 3 mM DTT, 0.01% BSA, 1 unit of GAPDH, and ca. 0.8 nM wild-type *Tbb*TIM.

The values of k_{cat} and K_{m} for mutant *Tbb*TIM-catalyzed isomerization of GAP or DHAP were determined from the fit to the Michaelis–Menten equation of initial velocities (v_i) determined at varying concentrations of substrate. The arsenate dianion used with the glyceraldehyde 3-phosphate dehydrogenase coupling enzyme in the assay for TIM-catalyzed isomerization of DHAP is a competitive inhibitor of wild-type *Tbb*TIM with $K_i = 4.6\text{ mM}$.⁴¹ Values for k_{cat} , K_{m} , and K_i for mutant *Tbb*TIM-catalyzed reaction of DHAP were determined from the nonlinear least-squares fit to eq 1 of initial velocities determined at varying concentrations of arsenate dianion and DHAP.

$$\frac{v_i}{[E]} = \frac{k_{\text{cat}}[\text{DHAP}]}{K_{\text{m}}(1 + [\text{HOAsO}_3^{2-}]/K_i) + [\text{DHAP}]} \quad (1)$$

^1H NMR Analyses. ^1H NMR spectra at 500 MHz were recorded in D_2O at 25 $^\circ\text{C}$ using a Varian Unity Inova 500 spectrometer that was shimmed to give a line width ≤ 0.7 Hz for each peak of the doublet due to the C-1 proton of GAP hydrate or ≤ 0.5 Hz for the most downfield peak of the doublet due to the C-1 proton of $[1\text{-}^{13}\text{C}]$ -GA hydrate. Spectra (16–64 transients) were obtained using a sweep width of 6000 Hz, a pulse angle of 90° , an acquisition time of 6 s and a relaxation delay of 60 s ($>5T_1$) for experiments on the TIM-catalyzed isomerization of GAP in D_2O or 120 s ($>8T_1$) for experiments on the TIM-catalyzed reaction of $[1\text{-}^{13}\text{C}]$ -GA in D_2O .^{33,38} It was shown in a control experiment with GAP that identical relative peak areas for substrate and product protons were observed for spectra determined using the long 120 s and the shorter 60 s delay time. Baselines were subjected to a first-order drift correction before determination of peak areas. Chemical shifts are reported relative to HOD at 4.67 ppm.

Isomerization of GAP in D_2O . The yields of the products of I172A and L232A mutant *Tbb*TIM-catalyzed reaction of GAP in D_2O at 25 $^\circ\text{C}$ were determined by ^1H NMR analysis, as described in studies on wild-type TIM.^{33,39} The enzyme was exhaustively dialyzed at 7 $^\circ\text{C}$ against 40 mM imidazole (70% free base) in D_2O at pD 7.9 and $I = 0.1$ (NaCl). The reaction was initiated by adding enzyme to give a final solution that contained 5 or 10 mM GAP, 20 mM imidazole (pD 7.9 at $I = 0.1$, NaCl), and 3.4 nM L232A *Tbb*TIM or 65 nM I172A *Tbb*TIM in a volume of 750 μL . The reactions at 25 $^\circ\text{C}$ were monitored by ^1H NMR spectroscopy. Spectra (16 transients) were recorded continuously during the reaction until the conversion of 80–90% of GAP to products. The peak areas were normalized using the signal for the C-(4,5) protons of the imidazole buffer as an internal standard. The fraction of the remaining substrate GAP (f_{GAP}) and the fractional product yields were determined from the integrated areas of the appropriate ^1H NMR signals, as described in earlier work.³³

Reactions of $[1\text{-}^{13}\text{C}]$ -GA in D_2O . The yields of the I172V, I172A, and L232A mutant *Tbb*TIM-catalyzed reactions of $[1\text{-}^{13}\text{C}]$ -GA in the presence or absence of HPO_3^{2-} in D_2O at 25 $^\circ\text{C}$ were determined by ^1H NMR analyses as described in earlier work.^{38,39} The enzyme was exhaustively dialyzed at 7 $^\circ\text{C}$ against 30 mM imidazole (20% free base, pD 7.0) in D_2O ($I = 0.024$ or 0.1 (NaCl)). The reactions in the absence of phosphite were initiated by adding enzyme to give a final solution that contained 20 mM $[1\text{-}^{13}\text{C}]$ -GA, 20 mM imidazole (20% free base, pD 7.0, $I = 0.1$ (NaCl)), and enzyme [0.16–0.34 mM L232A *Tbb*TIM; 0.4 mM I172V *Tbb*TIM; 0.3–0.7 mM I172A *Tbb*TIM] in a volume of 850 μL . The reactions in the presence of HPO_3^{2-} were initiated by adding enzyme to give a final solution that contained 20 mM $[1\text{-}^{13}\text{C}]$ -GA, 20 mM imidazole (20% free base, pD 7.0), 1–40 mM HPO_3^{2-} (50% dianion, pD 7.0), and enzyme [1–50 μM L232A or I172V *Tbb*TIM; 150–700 μM I172A *Tbb*TIM] in a volume of 850 μL ($I = 0.1$). In every case, 750 μL of the reaction mixture was transferred to an NMR tube, the ^1H NMR spectrum was recorded immediately, and spectra were then recorded at regular intervals. The remaining solution was incubated at 25 $^\circ\text{C}$, and the activity of TIM toward catalysis of isomerization of GAP was monitored. No significant loss in activity of TIM was observed during any of these reactions. At the end of each NMR experiment, the protein was removed by ultrafiltration, and the solution pD was

Chart 1

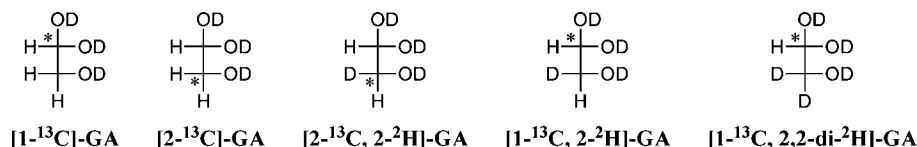


Table 1. Kinetic Parameters for the Isomerization Reactions of GAP and DHAP Catalyzed by TIM from Chicken Muscle, from *Trypanosoma brucei brucei*, and by Mutant Enzymes^a

TIM	GAP			DHAP			
	k_{cat}^b (s ⁻¹)	K_m^b (M)	$k_{\text{cat}}/K_m^{b,c}$ (M ⁻¹ s ⁻¹)	k_{cat}^d (s ⁻¹)	K_m^d (mM)	k_{cat}/K_m^d (M ⁻¹ s ⁻¹)	K_i^d (mM, arsenate)
WT <i>Tbb</i> ^e	2100	2.5×10^{-4}	8.4×10^6 (1.7×10^8)	300	7.0×10^{-4}	4.3×10^5	4.6 ^f
I172A <i>Tbb</i>	12	1.5×10^{-4}	8.0×10^4 (1.6×10^6)	17	3.7×10^{-3}	4.6×10^3	8.6
L232A <i>Tbb</i> ^g	220	1.4×10^{-4}	1.5×10^6 (3.0×10^7)	4.7	7.7×10^{-5}	6.1×10^4	4.6
I172V <i>Tbb</i>	225	5.8×10^{-5}	3.9×10^6 (7.8×10^7)	65	2.0×10^{-4}	3.2×10^5	4.5
WT chicken ^h	8300	4.2×10^{-4}	2.0×10^7	600	6.5×10^{-4}	9.2×10^5	11
E16SD chicken ^h	4.2	7.8×10^{-5}	5.4×10^4	4.1	1.2×10^{-3}	3.4×10^3	12
E16SD/S96P chicken ^h	68	6.6×10^{-5}	1.0×10^6	3.4	5.3×10^{-5}	6.4×10^4	2.1

^aUnder standard assay conditions: 30 mM TEA, pH 7.5, and 25 °C ($I = 0.1$, NaCl). In most cases, the variation in the values of k_{cat} and K_m determined in different experiments is less than $\pm 15\%$. ^bDetermined from the fit to the Michaelis–Menten equation of initial velocities (v_i) determined at ≥ 8 concentrations of GAP. ^cThe values in parentheses are calculated for catalysis of the reactive carbonyl form of GAP, which is present as 4% of the total substrate.⁴² ^dDetermined from the fit of the initial velocities (v_i) to eq 1. The concentration of arsenate was held constant as values of v_i were determined at eight different DHAP concentrations. This was repeated for a total of three fixed arsenate concentrations between 2 and 15 mM. ^eData from ref 39, unless noted otherwise. ^fData from ref 41. ^gData from ref 31. ^hData from ref 43. Conditions: 100 mM TEA, pH 7.5, 30 °C ($I = 0.1$).

determined. There was no significant change in pD during any of these reactions.

The observed ¹H NMR peak areas for the reaction products were normalized, as described in previous work, using the signal due to the C-(4,5) protons of imidazole or the upfield peak of the doublet due to the P–H proton of phosphite as an internal standard.³⁸ The fraction of the substrate $[1-^{13}\text{C}]\text{-GA}$ remaining and the fractional yields of the identifiable reaction products $[2-^{13}\text{C}]\text{-GA}$, $[2-^{13}\text{C}, 2\text{-}^2\text{H}]\text{-GA}$, $[1-^{13}\text{C}, 2\text{-}^2\text{H}]\text{-GA}$, and $[1-^{13}\text{C}, 2,2\text{-di-}^2\text{H}]\text{-GA}$ (Chart 1) were determined from the integrated areas of the relevant ¹H NMR signals for these compounds as described in earlier work.^{38,39} The disappearance of 30–70% $[1-^{13}\text{C}]\text{-GA}$ was monitored, and product yields were determined over the first ca. 20–30% of the reaction.

Observed first-order rate constants, k_{obs} (s⁻¹), for the reactions of $[1-^{13}\text{C}]\text{-GA}$ were determined from the slopes of linear semilogarithmic plots of reaction progress against time (eq 2), where f_s is the fraction of the substrate $[1-^{13}\text{C}]\text{-GA}$ remaining at time t . Observed second-order rate constants, $(k_{\text{cat}}/K_m)_{\text{obs}}$ (M⁻¹ s⁻¹), for the TIM-catalyzed reaction of $[1-^{13}\text{C}]\text{-GA}$ were determined from the values of k_{obs} using eq 3, where $f_{\text{hyd}} = 0.94$ is the fraction of $[1-^{13}\text{C}]\text{-GA}$ present as the hydrate.²⁰

$$\ln f_s = -k_{\text{obs}}t \quad (2)$$

$$(k_{\text{cat}}/K_m)_{\text{obs}} = \frac{k_{\text{obs}}}{(1 - f_{\text{hyd}})[\text{TIM}]} \quad (3)$$

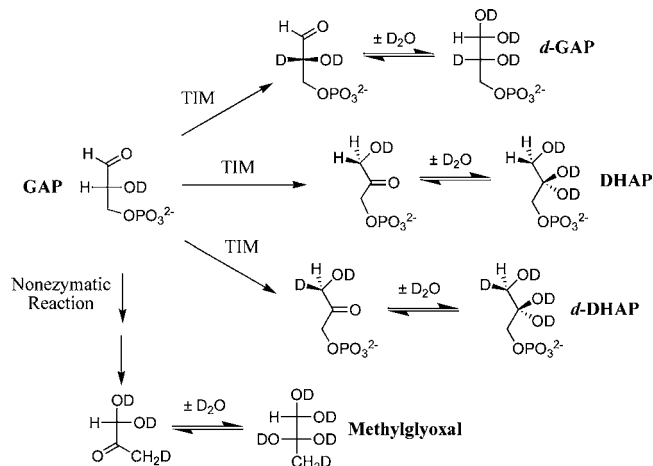
RESULTS

The kinetic parameters for wild-type and I172A, I172V, and L232A mutant TIM-catalyzed isomerization of GAP and DHAP, determined at pH 7.5 and 25 °C ($I = 0.1$, NaCl), are reported in Table 1. Arsenate is a required activator of glyceraldehyde 3-phosphate dehydrogenase, which was used as the coupling enzyme in assays of TIM-catalyzed isomerization of DHAP. Table 1 also reports the values of K_i for arsenate inhibition of this TIM-catalyzed reaction. The values of k_{cat}/K_m were calculated using the total concentration of GAP in the enzyme assay. However, GAP exists largely (96%) in the hydrated form, and TIM is specific for the carbonyl form of this substrate (4%).⁴²

The values for k_{cat}/K_m calculated for catalysis of the reactive carbonyl form of GAP are given in parentheses in Table 1.

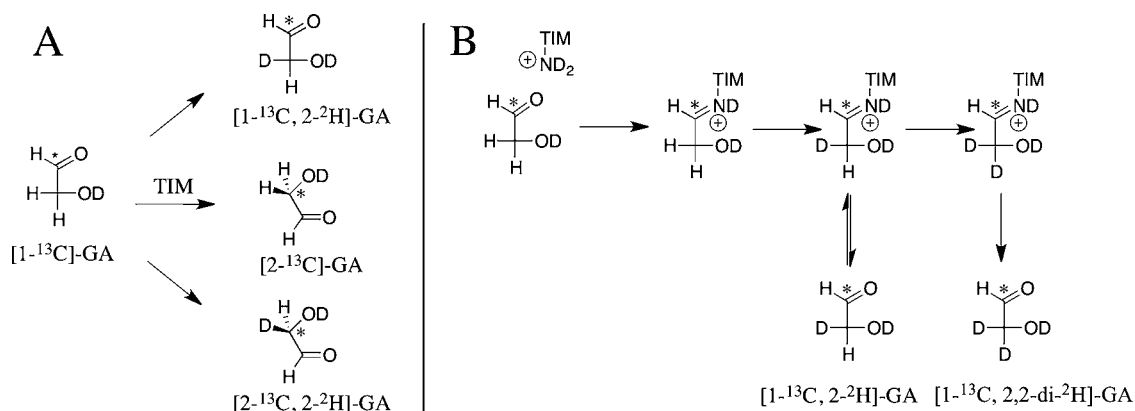
TIM-Catalyzed Isomerization of GAP in D₂O. The disappearance of GAP and the appearance of the products of its nonenzymatic and TIM-catalyzed reactions in D₂O (Scheme

Scheme 3



3) at pD 7.9 (20 mM imidazole) and 25 °C were monitored by ¹H NMR spectroscopy.^{17,33,39} Methylglyoxal is the product of the nonenzymatic elimination reaction of GAP (Scheme 3).⁹ The observed fractional product yields, $(f_p)_{\text{obs}}$, were calculated as the ratio $A_p/\sum A_p$, where A_p is the normalized ¹H NMR peak area of a single product proton and $\sum A_p$ is the sum of the normalized peak areas of single protons for every reaction product (eq 4). Values of $(f_p)_{\text{obs}}$ were determined at 4–6 different times over the first 6–8 h of the reaction, during which time >50% of GAP was consumed. The thermodynamically

Scheme 4



avored TIM-catalyzed conversion of *d*-GAP to *d*-DHAP results in <10% decreases and increases, respectively, in the apparent yields of these products.^{33,39} Values of f_T (Table 2) were determined as the *y*-intercept of linear plots (not shown) of $(f_P)_{\text{obs}}$ against the reaction time.^{33,39} The values of f_E (eqs 5–7) reported in Table 2 are the yields calculated as a fraction of the three products of the TIM-catalyzed reactions of GAP (Scheme 3).

$$(f_P)_{\text{obs}} = \frac{A_P}{A_{\text{DHAP}} + A_{d\text{-DHAP}} + A_{d\text{-GAP}} + A_{\text{MG}}} \quad (4)$$

$$(f_{d\text{-GAP}})_E = \frac{f_{d\text{-GAP}}}{f_{d\text{-GAP}} + f_{\text{DHAP}} + f_{d\text{-DHAP}}} \quad (5)$$

$$(f_{\text{DHAP}})_E = \frac{f_{\text{DHAP}}}{f_{d\text{-GAP}} + f_{\text{DHAP}} + f_{d\text{-DHAP}}} \quad (6)$$

$$(f_{d\text{-DHAP}})_E = \frac{f_{d\text{-DHAP}}}{f_{d\text{-GAP}} + f_{\text{DHAP}} + f_{d\text{-DHAP}}} \quad (7)$$

TIM-Catalyzed Reaction of $[1-^{13}\text{C}]\text{-GA}$ in D_2O . The mutant *Tbb*TIM-catalyzed reactions of $[1-^{13}\text{C}]\text{-GA}$ in D_2O were monitored by ^1H NMR spectroscopy.³⁸ The experimental results provide both the kinetic parameters for the TIM-catalyzed reaction of $[1-^{13}\text{C}]\text{-GA}$ and the yields of the reaction products (Chart 1). The product yields were determined at four different times during the first 20–30% of the reaction of $[1-^{13}\text{C}]\text{-GA}$ and are invariant ($\pm 5\%$) over this time. The disappearance of $[1-^{13}\text{C}]\text{-GA}$ was monitored for 30–70% of the reaction. The observed second-order rate constants $(k_{\text{cat}}/K_m)_{\text{obs}}$ ($\text{M}^{-1} \text{s}^{-1}$) for the TIM-catalyzed reaction of $[1-^{13}\text{C}]\text{-GA}$ were determined from the values of k_{obs} using eq 3.^{20,38} Values of (k_{cat}/K_m) for reactions at the active site of TIM were determined using eq 8, where f_E is the sum of the fractional yields of $[1-^{13}\text{C}, 2-^2\text{H}]\text{-GA}$, $[2-^{13}\text{C}]\text{-GA}$, and $[2-^{13}\text{C}, 2-^2\text{H}]\text{-GA}$ from TIM-catalyzed reactions of $[1-^{13}\text{C}]\text{-GA}$ (Scheme 4A).

L232A Mutant. The yields of the products of the L232A mutant *Tbb*TIM-catalyzed reactions of $[1-^{13}\text{C}]\text{-GA}$ in D_2O at pD 7.0 (20 mM imidazole, $I = 0.1$, NaCl) and 25 °C in the absence or the presence of HPO_3^{2-} are reported in Table 3. Only $[1-^{13}\text{C}, 2-^2\text{H}]\text{-GA}$, $[2-^{13}\text{C}]\text{-GA}$, and $[2-^{13}\text{C}, 2-^2\text{H}]\text{-GA}$ from reactions at the enzyme active site (Scheme 4A) were observed ($f_E = 1.0$, eq 8). Figure 3A (●) shows a plot of the increase, with increasing $[\text{HPO}_3^{2-}]$, in the second order-rate constant (k_{cat}/K_m) for L232A mutant TIM-catalyzed reaction of the carbonyl

Table 2. Product Yields, Expressed as Mole Fractions, and the Derived Product Rate Constant Ratios for Reaction of GAP in D_2O Catalyzed by Wild-type and Mutant Forms of *Tbb*TIM at 25 °C^a

TIM		fractional product yield ^b			MG
		DHAP	<i>d</i> -DHAP	<i>d</i> -GAP	
L232A TIM ^c	f_T ^d	0.036	0.75	0.086	0.12
	f_E ^e	0.041	0.86	0.098	
I172A TIM ^f	f_T ^d	0.12	0.33	0.45	0.10
	f_E ^e	0.13	0.37	0.50	
wild-type <i>Tbb</i> TIM ^g	f_E	0.40 ± 0.02	0.37 ± 0.02	0.22 ± 0.002	

TIM	rate constant ratio ^h	
	$k_{\text{ex}}/(k_{\text{C1}})_H$	$(k_{\text{C1}})_D/(k_{\text{C2}})_D$
L232A TIM	23	8.8
I172A TIM	6.7	0.74
wild-type <i>Tbb</i> TIM	1.5	1.7

^aFor the reaction of GAP at pD 7.9 (20 mM imidazole) and $I = 0.1$ (NaCl). ^bThe product yields (Scheme 3) were determined at 4–6 different times over a 6–8 h reaction time. ^cFor the reaction of 5 mM GAP catalyzed by 3.4 nM *Tbb* L232A TIM. ^dThe yields, f_T , reported in this table were determined as the *y*-intercept of linear plots of $(f_P)_{\text{obs}}$ (eq 4) against time.³³ The product yields determined in different experiments carried out under the same reaction conditions are typically reproducible to better than 5%.^{17,33,39} ^eFractional product yields for the TIM-catalyzed reactions (eqs 5–7). ^fFor the reaction of 5 mM GAP catalyzed by 65 nM *Tbb* I172A TIM. ^gData from ref 39. ^hThe ratios of rate constants, defined in Figure 4, calculated from the ratios of product yields as described in the text.

form of $[1-^{13}\text{C}]\text{-GA}$ that was reported in an earlier preliminary communication.³¹

$$\left(\frac{k_{\text{cat}}}{K_m}\right) = \left(\frac{k_{\text{cat}}}{K_m}\right)_{\text{obs}} f_E \quad (8)$$

I172V Mutant. The yield of the products of the I172V mutant *Tbb*TIM-catalyzed reactions of $[1-^{13}\text{C}]\text{-GA}$ in D_2O at pD 7.0 (20 mM imidazole, $I = 0.1$, NaCl) and 25 °C in the absence or the presence of HPO_3^{2-} are reported in Table 3. No $[1-^{13}\text{C}, 2,2\text{-di-}^2\text{H}]\text{-GA}$ from a nonspecific protein-catalyzed reaction (Scheme 4B) was detected for the relatively fast reactions in the presence of HPO_3^{2-} ($f_E = 1.0$). A 25% yield of $[1-^{13}\text{C}, 2,2\text{-di-}^2\text{H}]\text{-GA}$ was observed for the slow reaction in the absence of HPO_3^{2-} . The total yield of all of the reaction products from Chart 1 was 70%, and the yield of the products for Scheme 4A was 45% ($f_E = 0.45$).

Table 3. Product Yields, Expressed as Mole Fractions, from the Reactions of [1-¹³C]-GA Catalyzed by Mutant *Tbb*TIMs in the Absence and Presence of Phosphite Dianion in D₂O at 25 °C^a

[HPO ₃ ²⁻]/mM	[2- ¹³ C]-GA	[2- ¹³ C,2- ² H]-GA	[1- ¹³ C,2- ² H]-GA	[1- ¹³ C,2,2-di- ² H]-GA
TIM mutant L232A ^b				
0	0.01	0.45 ± 0.02	0.47 ± 0.02	0
2.4	0.01 ± 0.001	0.50 ± 0.05	0.50 ± 0.03	0
5	0.01 ± 0.001	0.50 ± 0.01	0.49 ± 0.02	0
10	0.01 ± 0.001	0.47 ± 0.01	0.52 ± 0.02	0
15	0.01 ± 0.001	0.47 ± 0.02	0.52 ± 0.01	0
20	0.01 ± 0.001	0.48 ± 0.02	0.51 ± 0.02	0
avg ^c	0.01 ± 0.001	0.48 ± 0.02	0.51 ± 0.02	
TIM mutant I172V ^d				
0	0.02 (0.04) ^e	0.18 (0.40) ^e	0.25 (0.55) ^e	0.25
5	0.12	0.62	0.26	0
10	0.13	0.63	0.24	0
15	0.12	0.62	0.26	0
20	0.14	0.65	0.21	0
avg ^c	0.13 ± 0.01	0.63 ± 0.01	0.24 ± 0.02	
TIM mutant I172A ^f				
0	0 ^g	0 ^g	0.15 ± 0.02	0.38 ± 0.08
5	0.02 ± 0.001	0.26 ± 0.03	0.30 ± 0.05	0.14 ± 0.04
10	0.02 ± 0.001	0.23 ± 0.02	0.29 ± 0.05	0.14 ± 0.06
15	0.02 ± 0.001	0.27 ± 0.03	0.32 ± 0.02	0.18 ± 0.06
20	0.02 ± 0.001	0.25 ± 0.04	0.29 ± 0.07	0.17 ± 0.02
avg ^c	0.02 ± 0.001	0.25 ± 0.02	0.30 ± 0.02	
WT <i>Tbb</i> TIM HPO ₃ ²⁻ activated reactions ^h				
	0.13	0.63	0.24	

^aFor reactions of 20 mM [1-¹³C]-GA at pD 7.0 and $I = 0.1$ (NaCl). ^bFractional yields of the products of L232A *Tbb*TIM-catalyzed reactions of [1-¹³C]-GA. The quoted errors originate from the product yields from two different experiments. ^cAverage product yields for the phosphite dianion-activated reaction of [1-¹³C]-GA. ^dFractional yields of the products of I172V *Tbb*TIM-catalyzed reactions of [1-¹³C]-GA. ^eFractional yields of [2-¹³C]-GA, [2-¹³C,2-²H]-GA, and [1-¹³C,2-²H]-GA from reaction at the enzyme active site (Scheme 4A). ^fFractional yields of the products of I172A *Tbb*TIM-catalyzed reactions of [1-¹³C]-GA. The quoted errors originate from the product yields from at least two different experiments. ^gNot detected. ^hData from ref 39.

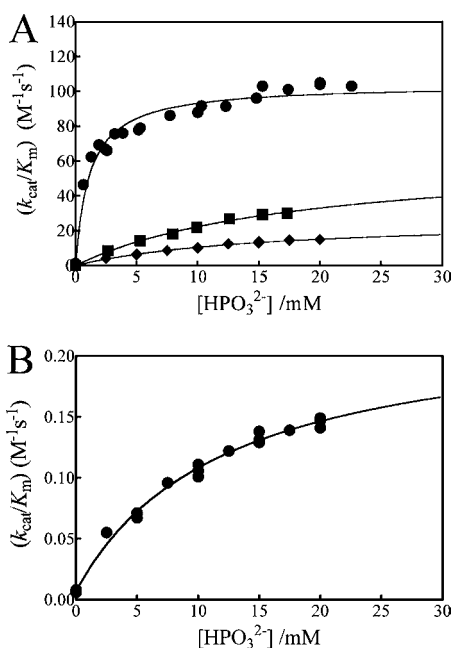


Figure 3. Dependence of the second-order rate constants (k_{cat}/K_m) for the TIM-catalyzed turnover of the carbonyl form of [1-¹³C]-GA in D₂O on the concentration of HPO₃²⁻ at pD 7.0 and 25 °C ($I = 0.1$, NaCl). The data were fit to eq 9 derived for the model shown in Scheme 5: (A) (●) L232A *Tbb*TIM, (■) wild-type *Tbb*TIM,³⁹ (◆) I172V *Tbb*TIM; (B) I172A *Tbb*TIM.

These product yields are similar to those determined for the unactivated wild-type *Tbb*TIM-catalyzed reactions of [1-¹³C]-GA.^{38,39} Figure 3A (◆) shows a plot of the increase, with increasing [HPO₃²⁻], in the second-order rate constant (k_{cat}/K_m) for I172V mutant TIM-catalyzed reaction of the carbonyl form of [1-¹³C]-GA.

I172A Mutant. The yield of the products of the I172A mutant TIM-catalyzed reactions of [1-¹³C]-GA in D₂O at pD 7.0 (20 mM imidazole, $I = 0.1$, NaCl) and 25 °C in the absence or the presence of HPO₃²⁻ are reported in Table 3. No [2-¹³C]-GA or [2-¹³C,2-²H]-GA from the isomerization of [1-¹³C]-GA were detected for the reaction in the absence of phosphite, but these products are observed for the phosphite dianion-activated enzyme-catalyzed reactions. The dianion activation is much weaker than for wild-type *Tbb*TIM, and a significant yield of [1-¹³C,2,2-di-²H]-GA from the nonspecific protein-catalyzed reaction was observed in all cases. The data in Table 3 were used to calculate a value of $f_E = (0.02 + 0.25 + 0.30) = 0.57 \pm 0.04$ for the sum of the yields of [2-¹³C]-GA, [2-¹³C,2-²H]-GA, and [1-¹³C,2-²H]-GA from reactions at the enzyme active site (Scheme 4A). Table 4 reports values of k_{obs} (s⁻¹, eq 2), (k_{cat}/K_m)_{obs} (M⁻¹s⁻¹, eq 3) and (k_{cat}/K_m) (M⁻¹s⁻¹, eq 8) for reactions in the presence of HPO₃²⁻. Most or all of the 15% yield of [1-¹³C,2-²H]-GA from the unactivated mutant TIM-catalyzed reaction is expected to form by the nonspecific pathway shown in Scheme 4B that gives an even larger 38% yield of [1-¹³C,2,2-di-²H]-GA. The yield of [1-¹³C,2-²H]-GA is observed to increase by 2-fold (from 15 to 30%) for the phosphite activated reactions, as the yield of [1-¹³C,2,2-di-²H]-GA from the nonspecific protein

Table 4. Kinetic Data for the Reaction of [1-¹³C]-GA Catalyzed by the I172A mutant of *Tbb*TIM in D₂O in the Absence and Presence of Phosphite Dianion in D₂O at 25 °C^a

[HPO ₃ ²⁻], mM	[TIM], M	k_{obs}^b (s ⁻¹)	$(k_{\text{cat}}/K_{\text{m}})_{\text{obs}}^c$ (M ⁻¹ s ⁻¹)	$(k_{\text{cat}}/K_{\text{m}})^d$ (M ⁻¹ s ⁻¹)
0	3.1 × 10 ⁻⁴	7.5 × 10 ⁻⁷	0.040	
0	3.4 × 10 ⁻⁴	1.1 × 10 ⁻⁶	0.055	
0	7.3 × 10 ⁻⁴	1.8 × 10 ⁻⁶	0.041	
2.5	4.0 × 10 ⁻⁴	2.3 × 10 ⁻⁶	0.096	0.055
5	3.4 × 10 ⁻⁴	2.5 × 10 ⁻⁶	0.12	0.071
5	6.9 × 10 ⁻⁴	5.3 × 10 ⁻⁶	0.13	0.071
5	3.3 × 10 ⁻⁴	2.4 × 10 ⁻⁶	0.12	0.067
7.5	4.0 × 10 ⁻⁴	4.1 × 10 ⁻⁶	0.17	0.096
10	1.7 × 10 ⁻⁴	2.0 × 10 ⁻⁶	0.19	0.11
10	3.4 × 10 ⁻⁴	3.6 × 10 ⁻⁶	0.18	0.10
10	4.0 × 10 ⁻⁴	4.6 × 10 ⁻⁶	0.19	0.11
12.5	4.0 × 10 ⁻⁴	5.3 × 10 ⁻⁶	0.22	0.12
15	1.7 × 10 ⁻⁴	2.4 × 10 ⁻⁶	0.23	0.13
15	2.1 × 10 ⁻⁴	3.1 × 10 ⁻⁶	0.24	0.14
15	4.0 × 10 ⁻⁴	5.6 × 10 ⁻⁶	0.23	0.13
17.5	4.0 × 10 ⁻⁴	5.9 × 10 ⁻⁶	0.24	0.14
20	1.5 × 10 ⁻⁴	2.40 × 10 ⁻⁶	0.26	0.15
20	1.7 × 10 ⁻⁴	2.7 × 10 ⁻⁶	0.26	0.15
20	1.7 × 10 ⁻⁴	2.5 × 10 ⁻⁶	0.25	0.14
20	4.0 × 10 ⁻⁴	6.4 × 10 ⁻⁶	0.26	0.15

^aFor reactions of 20 mM [1-¹³C]-GA at pD 7.0 and $I = 0.1$ (NaCl).

^bObserved first-order rate constant for the reaction of [1-¹³C]-GA calculated using eq 2. ^cObserved second-order rate constant for the TIM-catalyzed reaction of [1-¹³C]-GA calculated using eq 3. ^dSecond-order rate constant for the reactions of [1-¹³C]-GA, calculated (eq 8) from $(k_{\text{cat}}/K_{\text{m}})_{\text{obs}}$ and the average product yield $f_{\text{E}} = 0.57 \pm 0.04$ calculated from the product data reported in Table 3.

catalyzed reaction decreases from 38% to 14% (Table 3). This shows that most or all of the [1-¹³C,2-²H]-GA observed in these HPO₃²⁻-activated reactions forms by Scheme 4A. We cannot exclude the possibility of a ca. 5% yield of [1-¹³C,2,2-²H]-GA by Scheme 4B for reactions in the presence of the dianion activator. However, this uncertainty will not affect any conclusions from our discussion of the mechanism for dianion activation of the I172A mutant. Finally, we note that the initial 14% yield of [1-¹³C,2,2-di-²H]-GA observed for the reaction in the presence of 5 mM HPO₃²⁻ remains nearly constant as the concentration of the activator is increased to 20 mM. This shows that phosphite dianion acts both as an activator (Scheme 4A) and as a Brønsted-base catalyst of the protein-catalyzed reaction (Scheme 4B), as was proposed in an earlier study of reactions catalyzed by *c*TIM.³⁸

DISCUSSION

The conservative I172V mutation results in only a 2-fold decrease in $k_{\text{cat}}/K_{\text{m}}$ for isomerization of GAP that masks larger 4-fold and 9-fold decreases, respectively, in the individual kinetic parameters K_{m} and k_{cat} . The L232A and I172A mutations of *Tbb*TIM result in 6-fold and 100-fold decreases, respectively, compared with wild-type TIM, in $k_{\text{cat}}/K_{\text{m}}$ for isomerization of GAP and of DHAP (Table 1),³¹ but a 9-fold decrease and 5-fold increase in K_{m} for isomerization of DHAP. A larger enzyme activity is therefore observed for the L232A mutant, when the [DHAP] is low, and the relative velocity is determined by the 13-fold greater value of $k_{\text{cat}}/K_{\text{m}}$ for the L232A mutant, while a larger enzyme activity is observed for the I172A mutant when the

[DHAP] is saturating, and the relative velocity is determined by the 3.6-fold greater value of k_{cat} for the I172A mutant.

By comparison, a 12-fold decrease and 2-fold increase, respectively, compared with wild-type TIM, has been reported in the values of K_{m} for isomerization of DHAP catalyzed by the E165D/S96P and E165D mutants of TIM from chicken muscle (Table 1).⁴³ Consequently, the E165D mutant exhibits a 19-fold smaller $k_{\text{cat}}/K_{\text{m}}$ and a 1.2-fold larger k_{cat} compared with the E165D/S96P double mutant. These data suggest that the interactions between wild-type TIM and functionality at C-1 and C-2 are balanced in the binding of DHAP and GAP but that this balance is upset by L232A or E165D/S96P mutations that result in the stabilization of the complex to DHAP, while the I172A or E165D mutations result in a destabilization of this complex. These variations in K_{m} may reflect changes in the stabilization of the Michaelis complexes by hydrogen bond(s) to the substrate hydroxyl group. X-ray crystal structures determined for the E165D⁴⁴ and E165D/S96P⁴⁵ mutant enzymes show subtle changes in the positioning of catalytic residues at the enzyme active site, but the structures of the I172A and L232A mutants have not been determined.

Reactions of GAP in D₂O. Deprotonation of enzyme-bound GAP by the basic side chain of Glu-167 gives an intermediate and the protonated side chain. In a solvent of D₂O, the -H derived from substrate partitions between intramolecular transfer to form DHAP and essentially irreversible exchange with -D derived from solvent to form the D-labeled carboxylic acid. This -D then partitions between transfer to C-1 and to C-2 of the intermediate to form *d*-DHAP and *d*-GAP, respectively. Table 2 compares the yields of DHAP, *d*-DHAP, and *d*-GAP for wild-type TIM-catalyzed reactions of GAP in D₂O,³⁹ with the product yields for the reactions catalyzed by L232A and I172A mutant TIMs and reports values of the following rate constant ratios calculated from these product yields: (1) $k_{\text{ex}}/(k_{\text{C1}})_{\text{H}}$, the ratio of the sum of the yields of products that form after irreversible deuterium exchange (*d*-DHAP + *d*-GAP), and the product that forms by intramolecular transfer of -H (DHAP); (2) $(k_{\text{C1}})_{\text{D}}/(k_{\text{C2}})_{\text{D}}$, the ratio of the yields of *d*-DHAP and *d*-GAP that form by deuteration of the intermediate at C-1 and C-2, respectively.

If hydron transfer were directly to solvent D₂O, then the exchange between enzyme and solvent should be accelerated by general bases such as imidazole,⁴⁶ as has been documented for carbonic anhydrase.⁴⁷ However, there is no detectable imidazole catalysis of the exchange reaction with D₂O that results in an increase in the yields of *d*-DHAP and *d*-GAP.⁴⁸ This provides strong evidence that hydron transfer reactions of the reaction intermediate cannot involve the bulk aqueous solvent, and must therefore be with -D at the enzyme active site.⁴⁸ The experimental results are consistent with X-ray crystal structures of complexes between TIM and intermediate analogs, which show that these analogs are sequestered at an enzyme active site that is shielded from interaction with bulk solvent.^{21–23,27,49}

We propose the scheme shown in Figure 4 as a working model to rationalize the effects of the L232A, I172A, and other mutations on the product yields for reactions of GAP in D₂O. The exchange reaction (k_{ex}) is proposed to involve the -H from substrate and a pool with a minimal size of two -D, one derived from the substrate -OD and the second from the imidazole side chain of His-95. The presence of this side chain distinguishes this scheme from the simpler criss-cross mechanism that was proposed to explain the surprising effects of the H95Q mutation on the product yields for a reaction in tritiated water.¹²

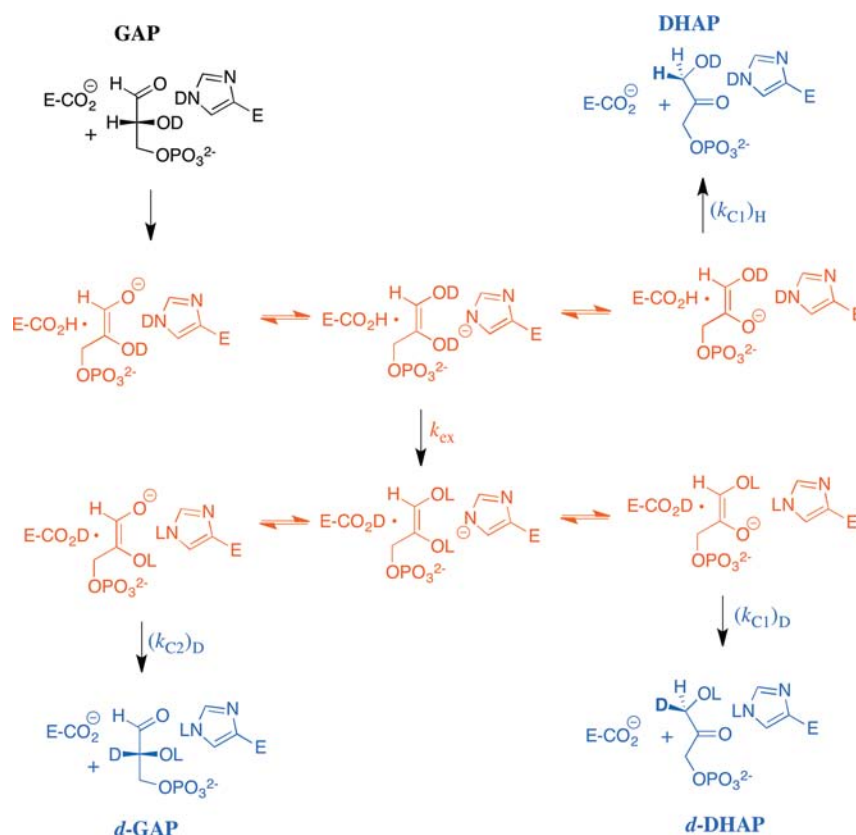


Figure 4. A minimal mechanism to rationalize the yields of the products of wild-type and mutant TIM-catalyzed reactions of GAP in D_2O . The $-H$ derived from substrate is exchanged with a pool of two $-D$ at the enzyme, the intermediate $-OD$ and the $-D$ at N-3 of the imidazole side chain of His-95. Fast transfer between four basic sites, the carboxylate of Glu-167, the two oxygen anions of the isomeric intermediates, and the N-3 imidazolates of His-95, scrambles a total of three hydrons. The steps that result in scrambling are not shown but are subsumed in the macroscopic rate constant k_{ex} . A mechanism, referred to as the criss-cross mechanism, has been proposed to explain the effects of the H95Q mutation on the product yields for reactions of GAP in 3H -labeled water.¹² In this mechanism (not shown), the $-H$ derived from substrate exchanges with a single hydron at the intermediate $-OD$, and there is no scrambling of hydrons at the C-1 and C-2 hydroxyl groups of the intermediate. In cases where a $>2/3$ yield of deuterium-labeled products is obtained, the substrate-derived hydron either undergoes fast irreversible exchange with deuterium at TIM or reversible exchange that scrambles a pool of >2 $-D$ at the enzyme active site.⁵⁰

The increase in $k_{ex}/(k_{C1})_H$ from 1.5 for wild-type *Tbb*TIM to 6.7 for the I172A mutant to 23 for L232A mutant (Table 2) shows that these mutations favor the D-exchange reaction compared with intramolecular transfer of $-H$. The $-CH_2CH_2CO_2^-/-CH_2CH_2CO_2H$ side chain of Glu-167 is presumably aligned optimally at the wild-type enzyme to react at both C-1 and C-2 of the bound substrate/intermediate.²¹ We suggest that substitution of the bulky hydrophobic side chain of Ile-172 or Leu-232 by a smaller methyl group results in movement of the glutamate side chain away from optimal alignment and favors proton transfer to the imidazolates of His-95 compared with carbon-2 of the reaction intermediate. The large 96% yield of *d*-DHAP and *d*-GAP observed for the L232A mutant *Tbb*TIM-catalyzed reaction requires either (a) the exchange step k_{ex} to be nearly irreversible, as was proposed for the criss-cross mechanism,¹² (b) the rapid scrambling of substrate $-H$ with a large pool of enzyme-bound $-D$, as proposed by Irwin Rose,⁵⁰ or (c) the mutations favoring direct exchange between the protonated side chain of Glu-167 and deuterium from bulk solvent. These different explanations will be difficult to distinguish.

The increase in $(k_{C1})_D/(k_{C2})_D$ (Figure 4) from 1.7 for wild-type *Tbb*TIM to 8.8 for the L232A mutant shows that this mutation also causes an increase in the reactivity of the intermediate for protonation at carbon-1, which is masked in

$k_{ex}/(k_{C1})_H$ by the even larger relative increase in k_{ex} . It is interesting that the L232A mutation causes a decrease both in K_m for DHAP compared with GAP, which is consistent with an increased binding affinity for DHAP, and in the relative reactivity of the enediolate phosphate for protonation at carbon-1 to form DHAP, compared with protonation at carbon-2 to form GAP. We propose that the interactions at the L232A mutant enzyme that stabilize the Michaelis complex to DHAP [perhaps a hydrogen bond to the carbon-1 hydroxyl] are also expressed at and stabilize the transition state for protonation of the intermediate to form DHAP.

Product Yields from the Reactions of $[1-^{13}C]$ -GA in D_2O .

The products of the reaction of $[1-^{13}C]$ -GA in D_2O form by essentially the same mechanism as shown in Figure 4 for the reactions of GAP. Deprotonation of $[1-^{13}C]$ -GA gives an enediolate and the protonated side chain,¹⁷ which partitions between intramolecular transfer of $-H$ to form $[2-^{13}C]$ -GA, and essentially irreversible exchange with D_2O to give $[2-^{13}C, 2-^2H]$ -GA and $[1-^{13}C, 2-^2H]$ -GA as the final reaction products (Scheme 4A). The conservative I172V mutation has no effect on the yields of the products of the phosphite dianion-activated reactions of $[1-^{13}C]$ -GA in D_2O (Table 3), while the yield of $[2-^{13}C]$ -GA from phosphite-activated reactions with intramolecular transfer of $-H$ decreases from 13% (wild-type *Tbb*TIM) to 2% (I172A mutant) or 1% (L232A mutant). This mirrors the change in the

yield of product DHAP (Table 2) of the reaction in D₂O with intramolecular transfer of -H, from 40% (wild-type *Tbb*TIM) to 13% (I172A mutant) to 4% (L232A mutant). The similar effects of these mutations on the product yields from reaction of the whole substrate GAP and from the reaction of substrate pieces [1-¹³C]-GA + HPO₃²⁻ in D₂O suggests a common explanation for these changes that was discussed above for the reaction of GAP.

An interesting question is whether the binding of HPO₃²⁻ to TIM affects the products of the TIM-catalyzed reactions of [1-¹³C]-GA. The same yields of [2-¹³C]-GA, [2-¹³C,2-²H]-GA, and [1-¹³C,2-²H]-GA (Scheme 4A) are observed from the wild-type *Tbb*TIM-catalyzed reactions of [1-¹³C]-GA in either the presence or the absence of phosphite dianion.^{38,39} In this case, the interactions between HPO₃²⁻ and TIM affect the rate of the reactions of [1-¹³C]-GA (Figure 3) but not the relative yields of the reaction products. Similarly, the same yield of products (Scheme 4A) is observed for the robust L232A TIM-catalyzed reactions of [1-¹³C]-GA in either the presence or the absence of phosphite dianion (Table 3).

The yields of products for the I172V TIM-catalyzed reactions of [1-¹³C]-GA in the absence of HPO₃²⁻ are different from the yields observed for the phosphite-activated reactions (Table 3). In particular, enzyme-bound HPO₃²⁻ causes the ratio of the yields of isomerization reaction products [2-¹³C]-GA and [2-¹³C,2-²H]-GA to change from 1/9 to 1/5 for reasons that we do not understand. The binding of HPO₃²⁻ to TIM results in an increase in the rate of the reactions shown in Scheme 4A, relative to the rate of the protein-catalyzed reactions (Scheme 4B). Therefore, the decrease in the yield of [1-¹³C,2-²H]-GA from reactions in the absence of phosphite dianion ($f_p = 0.55$) compared with its presence ($f_p = 0.24$) reflects the change in the fraction of the reaction that proceeds by the pathway shown in Figure 4B when the enzyme is strongly activated by phosphite dianion.^{20,38,51}

No [2-¹³C]-GA or [2-¹³C,2-²H]-GA is observed for the unactivated I172A TIM-catalyzed reactions of [1-¹³C]-GA. This strongly suggests that the observed products [1-¹³C,2-²H]-GA and [1-¹³C,2,2-di-²H]-GA form by *nonspecific* protein-catalyzed reactions (Scheme 4B). The binding of phosphite dianion to I172A TIM activates the enzyme for catalysis of the reactions of [1-¹³C]-GA to form the products shown in Scheme 4A. This might cause the partitioning of the reaction intermediate to change from the exclusive formation of [1-¹³C,2-²H]-GA in the unactivated reaction to the formation of a full complement of reaction products (Scheme 4A) for the phosphite-activated reaction. We consider this unlikely, because of the negligible or small effects of HPO₃²⁻ on the yields of the products of the wild-type, L232A, and I172V mutant *Tbb*TIM-catalyzed reactions.

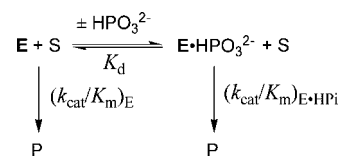
TbbTIM-Catalyzed Reactions of [1-¹³C]-GA in D₂O. Table 5 reports second-order rate constants (k_{cat}/K_m)_E (Scheme 5) for wild-type and mutant *Tbb*TIM-catalyzed reactions of [1-¹³C]-GA in the absence of phosphite dianion. These rate constants were calculated from the observed second-order rate constant using eq 8, where f_E is the yield of the products from reaction at the enzyme active site (Scheme 4A). Only the products from Scheme 4A were detected for the robust L232A mutant enzyme-catalyzed reaction ($f_E = 1.0$), for which a value of (k_{cat}/K_m)_E = 1.2 M⁻¹ s⁻¹ was determined. The value of (k_{cat}/K_m)_E = 0.03 M⁻¹ s⁻¹ for the I172V mutant TIM-catalyzed reaction was calculated from (k_{cat}/K_m)_{obs} = 0.063 M⁻¹ s⁻¹ and $f_E = 0.45$ (eq 8, Table 3). Finally, the I172A mutant shows no detectable [2-¹³C]-GA or [2-¹³C,2-²H]-GA from isomerization of [1-¹³C]-GA. The

Table 5. Kinetic Parameters for the Phosphite-Activated and Unactivated Reactions of [1-¹³C]-GA Catalyzed by Wild-type *Tbb* and Mutant TIMs in D₂O at 25 °C^a

TIM	(k_{cat}/K_m) _E (M ⁻¹ s ⁻¹)	(k_{cat}/K_m) _{E·HPi} (M ⁻¹ s ⁻¹)	K_d (mM)	(k_{cat}/K_m) _{E·HPi} / (k_{cat}/K_m) _E	(k_{cat}/K_d) _{E·HPi} / (k_{cat}/K_d) _E
WT <i>Tbb</i> ^b	0.07	64	19	900	3400
L232A ^c	1.2	100	1.2	80	83000
I172V	0.03	27	16	900	1700
I172A	<0.003 ^d	0.23	12	>77	20

^aFor reactions at pD 7.0 and $I = 0.1$ (NaCl). The kinetic parameters are defined in Scheme 5. ^bData from ref 39. ^cData from ref 31. ^dLimit calculated as described in the text.

Scheme 5



upper limit of (k_{cat}/K_m)_E < 0.003 M⁻¹ s⁻¹ was calculated from (k_{cat}/K_m)_{obs} = 0.045 M⁻¹ s⁻¹ (Table 4) assuming that no more than 1/2 of the observed 15% yield of [1-¹³C, 2-²H]-GA forms by a reaction at the enzyme active site ($f_E < 0.075$, eq 8).

Phosphite Activation of *Tbb*TIM-Catalyzed Reactions of [1-¹³C]-GA in D₂O. The effect of increasing [HPO₃²⁻] on (k_{cat}/K_m) for the reactions of [1-¹³C]-GA catalyzed by wild-type (■), I172V (◆), and L232A (●) *Tbb*TIM is shown in Figure 3A. Figure 3B shows the effect of increasing [HPO₃²⁻] on (k_{cat}/K_m) for reactions catalyzed by the I172A mutant. These data were fit to eq 9 derived for Scheme 5.²⁰ In Scheme 5, [1-¹³C]-GA undergoes a TIM-catalyzed reaction (E) with the second-order rate constant (k_{cat}/K_m)_E. TIM also undergoes conversion to the activated complex E·HPO₃²⁻ (K_d) that catalyzes the reaction of [1-¹³C]-GA with the second-order rate constant (k_{cat}/K_m)_{E·HPi}.²⁰ The values of (k_{cat}/K_m)_E from Table 5 were used in nonlinear least-squares fitting of the data to eq 9 to obtain the values for (k_{cat}/K_m)_{E·HPi} and K_d reported in Table 5.

$$\begin{aligned}
 \left(\frac{k_{\text{cat}}}{K_m}\right) &= \left(\frac{K_d}{K_d + [\text{HPO}_3^{2-}]}\right) \left(\frac{k_{\text{cat}}}{K_m}\right)_E \\
 &+ \left(\frac{[\text{HPO}_3^{2-}]}{K_d + [\text{HPO}_3^{2-}]}\right) \left(\frac{k_{\text{cat}}}{K_m}\right)_{\text{E} \cdot \text{HPi}} \quad (9)
 \end{aligned}$$

I172V Mutant. This conservative mutation results in only a 2-fold decrease in (k_{cat}/K_m)_E and (k_{cat}/K_m)_{E·HPi} (Scheme 5) for deprotonation of [1-¹³C]-GA by E and by E·HPO₃²⁻, respectively, and no change in the 900-fold enzyme activation by phosphite dianion (Table 5). We conclude that the I172V mutation has a similar small effect on the kinetic parameters for the *Tbb*TIM-catalyzed reactions of the substrate pieces and on k_{cat}/K_m for catalysis of isomerization of the whole substrates GAP and DHAP (Table 1). It is interesting that the corresponding I170V mutation has in one case been noted as the cause of a TIM-deficiency in humans that gives rise to a genetic disease.⁵² Evidently, there are drastic physiological consequences associated with the minor effects of this mutation on the kinetic parameters for TIM.

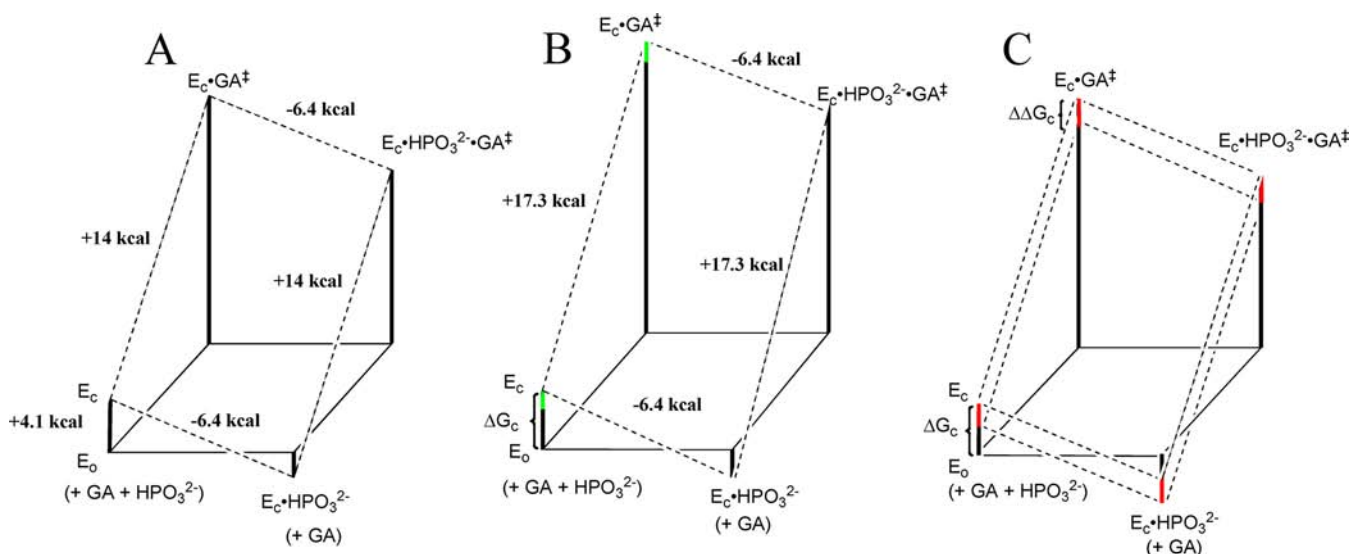


Figure 5. Free energy profiles for turnover of GA by free TIM (E_O) and by TIM that is saturated with HPO_3^{2-} ($E_C \cdot HPO_3^{2-}$) constructed using the kinetic parameters reported in Table 5. The profiles show the activation free energy changes calculated using the Eyring equation at 298 K for reactions catalyzed by wild-type and mutant forms of *Tbb*TIM. (A) Reactions catalyzed by wild-type *Tbb*TIM. The difference between the total intrinsic phosphite binding energy of -6.4 kcal/mol and $\Delta G^\circ = -2.3$ kcal/mol for binding of HPO_3^{2-} to the inactive open enzyme E_O to give the active closed liganded enzyme $E_C \cdot HPO_3^{2-}$ is attributed to $\Delta G_C = 4.1$ kcal/mol for the conformational change that converts E_O to E_C . (B) Reactions catalyzed by I172A mutant *Tbb*TIM. The overall barrier for conversion of $E_C \cdot HPO_3^{2-}$ to the transition state for reaction of GA is 3.3 kcal/mol higher than for the reaction catalyzed by wild-type *Tbb*TIM. The green bars show the uncertainty in the barrier to the unactivated reaction of GA, which was drawn using the upper limit of $(k_{cat}/K_m)_E < 0.003 \text{ M}^{-1} \text{ s}^{-1}$ (Table 5) and a lower limit calculated with the assumption that the total 6.4 kcal/mol intrinsic phosphite dianion binding energy is equal to that for wild-type *Tbb*TIM. (C) Reactions catalyzed by L232A mutant *Tbb*TIM. The red bars show the proposed effect of the L232A mutation on the barrier for the conformational change from E_O to E_C ($\Delta\Delta G_C$). A comparison of the reaction profiles for wild-type TIM (upper dashed lines) and the L232A mutant (lower dashed lines) shows the effect of this change in ΔG_C on the kinetic parameters for the reaction of the substrate pieces.

$K_m)_{E \cdot HP_i}/K_d$. In other words, mutations at the different sides of the hydrophobic clamp (Figure 2A,B) can result in an increase or a decrease in the enzymatic activity toward the catalyzed reactions of substrate pieces. We have not determined the X-ray crystal structures for these mutant enzymes that are required for a full structure-based explanation of the effects of the mutations determined in this work. However, the large body of existing structural data for TIM provides support for the following partial rationalization of these effects.

The ligand-driven conformational change of TIM results in a ca 2 Å shift of the carboxylate side chain of Glu-167 from a “swung-out” position to an active “swung-in” position (Figure 2A) that places the carboxylate anion in a hydrophobic cage and aligns the functional group to deprotonate the bound substrate (Figure 2B).^{21,22} A correlation has been observed between the magnitude of the falloff in the catalytic activity of mutant forms of TIM and the shift in the position of this side chain. For example, the 370-fold and 23-fold decreases, respectively, in k_{cat}/K_m for the E165D^{43,53} and S96P⁴³ mutants of *c*TIM are associated with 0.7 Å (E165D⁴⁴) and 0.4 Å (S96P⁴⁵) shifts in the position of the carboxylate side chain. The P168A mutation of *Tbb*TIM results in a 35-fold decrease in k_{cat}/K_m for isomerization of GAP, and the X-ray crystal structure for the mutant enzyme shows that the side chain for Glu-167 remains in the swung-out position at the enzyme-PGA complex.⁵⁴ We suggest, similarly, that the loop closure by I172A mutant TIM may not induce the full change in the position of the carboxylate side chain from the inactive “swung-out” to the active “swung-in” position.

Part of the barrier to conversion of E_O to E_C (ΔG_C) is probably desolvation of the solvent-exposed active-site of TIM that accompanies ligand binding and the closure of loop 6.⁵ The

I172A mutation creates space at the active site that might be occupied by water, with the following possible effects: (a) Solvating the anionic side chain of Glu-167. This would result in a decrease in side-chain reactivity for deprotonation of carbon, which leads to a decrease in $(k_{cat}/K_m)_E$ and $(k_{cat}/K_m)_{E \cdot HP_i}/K_d$. (b) A decrease in the contribution of the barrier to desolvation of the enzyme active site to ΔG_C for the enzyme conformational change. The I172A mutation results in decreases in the values of both $(k_{cat}/K_m)_{E \cdot HP_i}/K_d$ and $(k_{cat}/K_m)_E$ (Table 5) that are consistent with a decrease in the reactivity of TIM toward deprotonation of carbon. The value of K_C is defined by the ratio of these rate constants (eq 11),³¹ but the effect of this mutation on the rate constant ratio is uncertain, because it has only been possible to set limits for $(k_{cat}/K_m)_E$.

The 17-fold effect of the L232A mutation on $(k_{cat}/K_m)_E$ for the reaction of $[1-^{13}\text{C}]\text{-GA}$ might reflect a decrease in barrier to desolvation of E_O during its conversion to E_C . This would require that the effect of the mutation be expressed largely on K_C (eq 11) and that the effect on side chain basicity/reactivity be relatively small. This is difficult or impossible to reconcile with the proposed function of desolvation of E_O , which is to increase the side-chain basicity/reactivity. We suggest that the L232A mutation results in a decrease in ΔG_C because the mutation relieves steric interactions between the basic side chain of Glu-167 and the hydrophobic side chain of Leu-232 at the closed enzyme. We advise a healthy skepticism to this proposal, because the factors that control the rate and equilibrium constants for the complex ligand-driven conformational change are poorly understood. This process involves the movement of many atoms, the rotation of both peptide and side chain bonds, and the cleavage

and formation of several hydrogen bonds, any of which might be perturbed by the L232A mutation.^{4,29}

Catalysis of Isomerization of the Whole Substrate. The L232A mutation results in a contrasting 6-fold decrease in $k_{\text{cat}}/K_{\text{m}}$ for the TIM-catalyzed isomerization of the whole substrates GAP or DHAP (Table 1) and 17-fold and 24-fold increases, respectively, in $(k_{\text{cat}}/K_{\text{m}})_{\text{E}}$ and $(k_{\text{cat}}/K_{\text{m}})_{\text{E:HP}}/K_{\text{d}}$ for the reactions of GA and of GA + HPO_3^{2-} (Table 5). This shows that there are substantial differences in the processes that control the kinetic parameters for the reactions of the whole substrate and substrate pieces. We note that the increase in the concentration of E_{C} relative to E_{O} that was proposed to rationalize the effect of the mutation on $(k_{\text{cat}}/K_{\text{m}})_{\text{E}}$ for the reaction of GA is unlikely to result in an increase in $k_{\text{cat}}/K_{\text{m}}$ for isomerization of the whole substrate GAP, because this rate constant is at the diffusion-controlled limit.⁵⁵ A diffusion-limited reaction by the mechanism shown in Scheme 6 would require that conversion of the first-formed $\text{E}_{\text{O}}\cdot\text{GAP}$ complex to the active $\text{E}_{\text{C}}\cdot\text{GAP}$ complex and then to product be faster than dissociation of GAP from $\text{E}_{\text{O}}\cdot\text{GAP}$.

The observed decrease in $k_{\text{cat}}/K_{\text{m}}$ for isomerization of GAP catalyzed by the L232A mutant may be due to an increase in the chemical barrier to isomerization that we cannot easily rationalize. Alternatively, it might reflect an increase in the barrier to the formation and breakdown of a reactive encounter complex between TIM and substrate, since a substantial variation in these barriers has been observed for other enzyme-catalyzed reactions. For example, the value of $k_{\text{cat}}/K_{\text{m}}$ for yeast orotidine 5'-monophosphate decarboxylase-catalyzed decarboxylation of 5-fluoroorotidine 5'-monophosphate decreases with increasing solvent viscosity in the manner predicted for an encounter-limited reaction.⁵⁶ The value of $k_{\text{cat}}/K_{\text{m}} = 2.6 \times 10^7 \text{ M}^{-1} \text{ s}^{-1}$ for the catalyzed reaction in water is smaller than $k_{\text{cat}}/K_{\text{m}} = 3.8 \times 10^7$ for isomerization of the carbonyl form of GAP catalyzed by L232A *Tbb*TIM (Table 1). The Y208F mutation of *c*TIM results in the loss of an intraloop hydrogen bond to the backbone amide of Ala-176. The mutation leads to a 2000-fold decrease in $k_{\text{cat}}/K_{\text{m}}$ for isomerization of GAP, to a value that is well below the diffusion-controlled limit⁵⁷ but decreases with increasing solvent viscosity.⁵⁸ It was proposed that loop closure to trap the initial substrate complex is rate-determining for the Y208F mutant TIM-catalyzed reaction. We suggest, by analogy, that the decrease in $k_{\text{cat}}/K_{\text{m}}$ observed for the L232A mutant TIM-catalyzed reactions of GAP and DHAP reflects an increase in the kinetic barrier to conversion of the complex between open enzyme and ligand to the active closed form.

AUTHOR INFORMATION

Corresponding Author

jrichard@buffalo.edu

Notes

The authors declare no competing financial interest.

ACKNOWLEDGMENTS

We acknowledge the National Institutes of Health Grant GM39754 for generous support of this work. We thank Professor Gerald Koudelka for advice on the preparation of the I172A, I172V, and L232A mutants of *Tbb* TIM.

REFERENCES

- (1) Knowles, J. R.; Albery, W. J. *Acc. Chem. Res.* **1977**, *10*, 105–111.
- (2) Knowles, J. R. *Nature* **1991**, *350*, 121–124.
- (3) Knowles, J. R. *Philos. Trans. R. Soc. London, Ser. B* **1991**, *332*, 115–121.
- (4) Wierenga, R. K. *Cell. Mol. Life Sci.* **2010**, *67*, 3961–3982.
- (5) Richard, J. P. *Biochemistry* **2012**, *51*, 2652–2661.
- (6) Rieder, S. V.; Rose, I. A. *J. Biol. Chem.* **1959**, *234*, 1007–1010.
- (7) Orosz, F.; Olah, J.; Ovadi, J. *Biochim. Biophys. Acta, Mol. Basis Dis.* **2009**, *1792*, 1168–1174.
- (8) Orosz, F.; Olah, J.; Ovadi, J. *IUBMB Life* **2006**, *58*, 703–715.
- (9) Richard, J. P. *J. Am. Chem. Soc.* **1984**, *106*, 4926–4936.
- (10) Waley, S. G.; Miller, J. C.; Rose, I. A.; O'Connell, E. L. *Nature* **1970**, *227*, 181.
- (11) Miller, J. C.; Waley, S. G. *Biochem. J.* **1971**, *123*, 163–170.
- (12) Nickbarg, E. B.; Davenport, R. C.; Petsko, G. A.; Knowles, J. R. *Biochemistry* **1988**, *27*, 5948–5960.
- (13) Komives, E. A.; Chang, L. C.; Lolis, E.; Tilton, R. F.; Petsko, G. A.; Knowles, J. R. *Biochemistry* **1991**, *30*, 3011–3019.
- (14) Joseph-McCarthy, D.; Lolis, E.; Komives, E. A.; Petsko, G. A. *Biochemistry* **1994**, *33*, 2815–2823.
- (15) Lodi, P. J.; Chang, L. C.; Knowles, J. R.; Komives, E. A. *Biochemistry* **1994**, *33*, 2809–2814.
- (16) Go, M. K.; Amyes, T. L.; Richard, J. P. *J. Am. Chem. Soc.* **2010**, *132*, 13525–13532.
- (17) Go, M. K.; Koudelka, A.; Amyes, T. L.; Richard, J. P. *Biochemistry* **2010**, *49*, 5377–5389.
- (18) Malabanan, M. M.; Amyes, T. L.; Richard, J. P. *Curr. Opin. Struct. Biol.* **2010**, *20*, 702–710.
- (19) Amyes, T. L.; O'Donoghue, A. C.; Richard, J. P. *J. Am. Chem. Soc.* **2001**, *123*, 11325–11326.
- (20) Amyes, T. L.; Richard, J. P. *Biochemistry* **2007**, *46*, 5841–5854.
- (21) Jogl, G.; Rozovsky, S.; McDermott, A. E.; Tong, L. *Proc. Natl. Acad. Sci. U.S.A.* **2003**, *100*, 50–55.
- (22) Kursula, I.; Wierenga, R. K. *J. Biol. Chem.* **2003**, *278*, 9544–9551.
- (23) Alahuhta, M.; Wierenga, R. K. *Proteins: Struct., Funct., Bioinf.* **2010**, *78*, 1878–1888.
- (24) Nobel, M. E. M.; Zeelen, J. P.; Wierenga, R. K. *Proteins: Struct., Funct., Genet.* **1993**, *16*, 311–326.
- (25) Alber, T.; Banner, D. W.; Bloomer, A. C.; Petsko, G. A.; Phillips, D.; Rivers, P. S.; Wilson, I. A. *Philos. Trans. R. Soc. London, Ser. B* **1981**, *293*, 159–171.
- (26) Lolis, E.; Petsko, G. A. *Biochemistry* **1990**, *29*, 6619–6625.
- (27) Davenport, R. C.; Bash, P. A.; Seaton, B. A.; Karplus, M.; Petsko, G. A.; Ringe, D. *Biochemistry* **1991**, *30*, 5821–5826.
- (28) Pompliano, D. L.; Peyman, A.; Knowles, J. R. *Biochemistry* **1990**, *29*, 3186–3194.
- (29) Kursula, I.; Salin, M.; Sun, J.; Norledge, B. V.; Haapalainen, A. M.; Sampson, N. S.; Wierenga, R. K. *Protein Eng., Des. Sel.* **2004**, *17*, 375–382.
- (30) Wierenga, R. K.; Noble, M. E. M.; Vriend, G.; Nauche, S.; Hol, W. G. J. *J. Mol. Biol.* **1991**, *220*, 995–1015.
- (31) Malabanan, M. M.; Amyes, T. L.; Richard, J. P. *J. Am. Chem. Soc.* **2011**, *133*, 16428–16431.
- (32) Bergemeyer, H. U.; Haid, E.; Nelboeck-Hochstetter, M. U.S. Patent, 3,662,037, 1972.
- (33) O'Donoghue, A. C.; Amyes, T. L.; Richard, J. P. *Biochemistry* **2005**, *44*, 2610–2621.
- (34) Borchert, T. V.; Pratt, K.; Zeelen, J. P.; Callens, M.; Noble, M. E. M.; Opperdoes, F. R.; Michels, P. A. M.; Wierenga, R. K. *Eur. J. Biochem.* **1993**, *211*, 703–710.
- (35) Gasteiger, E.; Hoogland, C.; Gattiker, A.; Duvaud, S.; Wilkins, M. R.; Appel, R. D.; Bairoch, A. *Proteomics Protoc. Handb.* **2005**, 571–607.
- (36) Gasteiger, E.; Gattiker, A.; Hoogland, C.; Ivanyi, I.; Appel, R. D.; Bairoch, A. *Nucleic Acids Res.* **2003**, *31*, 3784–3788.
- (37) Glasoe, P. K.; Long, F. A. *J. Phys. Chem.* **1960**, *64*, 188–190.
- (38) Go, M. K.; Amyes, T. L.; Richard, J. P. *Biochemistry* **2009**, *48*, 5769–5778.
- (39) Malabanan, M. M.; Go, M. K.; Amyes, T. L.; Richard, J. P. *Biochemistry* **2011**, *50*, 5767–5779.
- (40) Plaut, B.; Knowles, J. R. *Biochem. J.* **1972**, *129*, 311–320.

- (41) Lambeir, A. M.; Opperdoes, F. R.; Wierenga, R. K. *Eur. J. Biochem.* **1987**, *168*, 69–74.
- (42) Trentham, D. R.; McMurray, C. H.; Pogson, C. I. *Biochem. J.* **1969**, *114*, 19–24.
- (43) Blacklow, S. C.; Knowles, J. R. *Biochemistry* **1990**, *29*, 4099–4108.
- (44) Joseph-McCarthy, D.; Rost, L. E.; Komives, E. A.; Petsko, G. A. *Biochemistry* **1994**, *33*, 2824–2829.
- (45) Zhang, Z.; Komives, E. A.; Sugio, S.; Blacklow, S. C.; Narayana, N.; Xuong, N. H.; Stock, A. M.; Petsko, G. A.; Ringe, D. *Biochemistry* **1999**, *38*, 4389–4397.
- (46) Eigen, M. *Angew. Chem., Int. Ed. Engl.* **1964**, *3*, 1–72.
- (47) Tu, C.; Paranawithana, S. R.; Jewell, D. A.; Tanhauser, S. M.; LoGrasso, P. V.; Wynns, G. C.; Laipis, P. J.; Silverman, D. N. *Biochemistry* **1990**, *29*, 6400–6405.
- (48) O'Donoghue, A. C.; Amyes, T. L.; Richard, J. P. *Org. Biomol. Chem.* **2008**, *6*, 391–396.
- (49) Zhang, Z.; Sugio, S.; Komives, E. A.; Liu, K. D.; Knowles, J. R.; Petsko, G. A.; Ringe, D. *Biochemistry* **1994**, *33*, 2830–2837.
- (50) Rose, I. A.; Fung, W. J.; Warms, J. V. B. *Biochemistry* **1990**, *29*, 4312–4317.
- (51) Go, M. K.; Malabanan, M. M.; Amyes, T. L.; Richard, J. P. *Biochemistry* **2010**, *49*, 7704–7708.
- (52) Arya, R.; Lalloz, M. R. A.; Bellingham, A. J.; Layton, D. M. *Hum. Mutat.* **1997**, *10*, 290–294.
- (53) Straus, D.; Raines, R.; Kawashima, E.; Knowles, J. R.; Gilbert, W. *Proc. Natl. Acad. Sci. U.S.A.* **1985**, *82*, 2272–2276.
- (54) Casteleijn, M. G.; Alahuhta, M.; Groebel, K.; El-Sayed, I.; Augustyns, K.; Lambeir, A.-M.; Neubauer, P.; Wierenga, R. K. *Biochemistry* **2006**, *45*, 15483–15494.
- (55) Blacklow, S. C.; Raines, R. T.; Lim, W. A.; Zamore, P. D.; Knowles, J. R. *Biochemistry* **1988**, *27*, 1158–1165.
- (56) Wood, B. M.; Chan, K. K.; Amyes, T. L.; Richard, J. P.; Gerlt, J. A. *Biochemistry* **2009**, *48*, 5510–5517.
- (57) Sampson, N. S.; Knowles, J. R. *Biochemistry* **1992**, *31*, 8482–8487.
- (58) Sampson, N. S.; Knowles, J. R. *Biochemistry* **1992**, *31*, 8488–8494.